

2-[(1*E*)-{[(Benzylsulfanyl)methanethioyl]amino}-imino)methyl]-6-methoxyphenol: crystal structure and Hirshfeld surface analysisEnis Nadia Md Yusof,^a Mukesh M. Jotani,^b Edward R. T. Tiekink^{c*} and Thahira B. S. A. Ravoo^{a‡}

Received 11 March 2016

Accepted 14 March 2016

Edited by W. T. A. Harrison, University of Aberdeen, Scotland

‡ Additional correspondence author, e-mail: thahira@upm.edu.my.

Keywords: crystal structure; hydrogen bonding; dithiocarbazate ester; Hirshfeld surface analysis.**CCDC reference:** 1465209**Supporting information:** this article has supporting information at journals.iucr.org/e^aDepartment of Chemistry, Faculty of Science, Universiti Putra Malaysia, 43400, UPM Serdang, Selangor Darul Ehsan, Malaysia, ^bDepartment of Physics, Bhavan's Sheth R. A. College of Science, Ahmedabad, Gujarat 380 001, India, and ^cResearch Centre for Crystalline Materials, Faculty of Science and Technology, Sunway University, 47500 Bandar Sunway, Selangor Darul Ehsan, Malaysia. *Correspondence e-mail: edwardt@sunway.edu.my

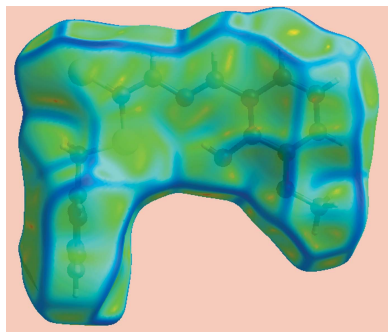
The title dithiocarbazate ester, C₁₆H₁₆N₂O₂S₂, comprises two almost planar residues, *i.e.* the phenyl ring and the remaining 14 non-H atoms (r.m.s. deviation = 0.0410 Å). These are orientated perpendicularly, forming a dihedral angle of 82.72 (5)°. An intramolecular hydroxy-O—H···N(imine) hydrogen bond, leading to an *S*(6) loop, is noted. An analysis of the geometric parameters is consistent with the molecule existing as the thione tautomer, and the conformation about the C=N bond is *E*. The thione S and imine H atoms lie to the same side of the molecule, facilitating the formation of intermolecular N—H···S hydrogen bonds leading to eight-membered {···HNCS}₂ synthons in the crystal. These aggregates are connected by phenyl-C—H···O(hydroxy) interactions into a supramolecular layer in the *bc* plane; these stack with no directional interactions between them. An analysis of the Hirshfeld surface confirms the nature of the intermolecular interactions.

1. Chemical context

Dithiocarbazate, NH₂NHC(=S)S[−], and more specifically substituted derivatives, have attracted the attention of researchers for decades (Ali & Livingstone, 1974). While a common motivation for investigating transition metal complexes of these anions relates to potential biological activity (Basha *et al.*, 2012; Vijayan *et al.*, 2015), including our own recent work (Yusof, Ravoo, Jamsari *et al.*, 2015; Yusof, Ravoo, Tiekink *et al.*, 2015), other motivations exist. Thus, recent studies have described the photo-catalytic production of hydrogen mediated by a conjugated nickel(II) bis-dithiocarbazate complex (Wise *et al.*, 2015). The use of a coumarin-based dithiocarbazate as a ratiometric and colorimetric chemosensor for cobalt(II) is another recent development (Liu *et al.*, 2015). In rationalizing the electronic structures of metal dithiocarbazates, a knowledge of the uncomplexed or 'free ligand' structure is most useful. In keeping with this notion and as a part of an on-going study of the structural chemistry of metal dithiocarbazates and their ligands, the title compound was prepared and characterized both crystallographically and by a Hirshfeld surface analysis.

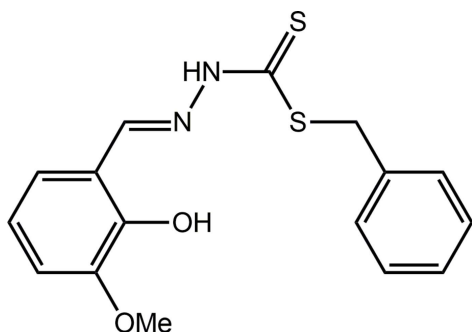
2. Structural commentary

The title compound, Fig. 1, comprises two almost planar regions, one being the phenyl ring, the other being the



OPEN ACCESS

remaining 14 non-hydrogen atoms. The maximum deviations from the least-squares plane through the latter plane, with a r.m.s. deviation = 0.0410 Å, are 0.0715 (15) for the O1 atom and −0.0796 (18) for atom C16. To a first approximation, the molecule can be described as having mirror symmetry with the 1,4-atoms of the terminal ring being bisected by the plane. Substantiating this description is the dihedral angle between the planes of 82.72 (5)°, indicating a very close to perpendicular relationship. The observed planarity in the larger fragment may be ascribed, in part, to the presence of an intramolecular hydroxy-O—H···N(imine) hydrogen bond (Table 1), which leads to the formation of an *S*(6) loop. The molecule exists in the thione tautomeric form. Consistent with this assignment, the thione C1=S2 bond length, *i.e.* 1.670 (2) Å, is considerably shorter than the thiol C1—S1 and, especially, C2—S1 bonds of 1.749 (2) and 1.817 (2) Å, respectively. The conformation about the C=N bond is *E*, and the amine-N—H atom is flanked on either side by the thione-S and imine-H atoms.



3. Supramolecular features

The most prominent feature of the packing of the title compound is the formation of centrosymmetric, eight-membered {···HNCS}₂ synthons through the agency of thioamide-N—H···S(thione) hydrogen bonds, Table 1. The dimeric aggregates are connected by phenyl-C—H···O(hy-

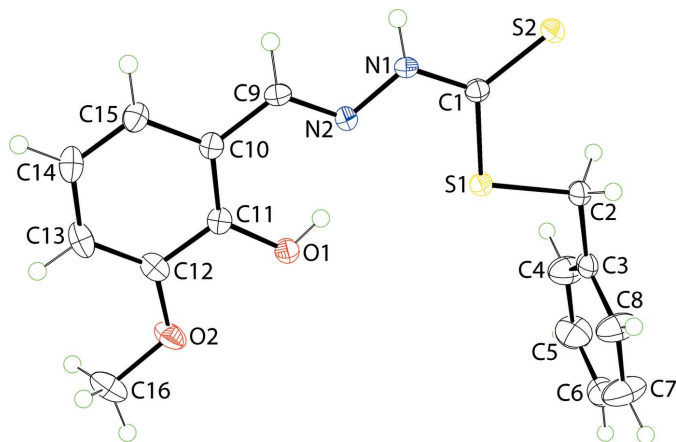


Figure 1

The molecular structure of the title compound, showing the atom-labelling scheme and displacement ellipsoids at the 50% probability level.

Table 1

Hydrogen-bond geometry (Å, °).

<i>D</i> —H··· <i>A</i>	<i>D</i> —H	H··· <i>A</i>	<i>D</i> ··· <i>A</i>	<i>D</i> —H··· <i>A</i>
O1—H1O···N2	0.84 (2)	1.90 (2)	2.639 (2)	146 (2)
N1—H1N···S2 ⁱ	0.88 (2)	2.47 (2)	3.3351 (18)	168 (2)
C6—H6···O1 ⁱⁱ	0.95	2.51	3.453 (3)	170

Symmetry codes: (i) $-x + \frac{1}{2}, -y + \frac{3}{2}, -z + 1$; (ii) $-x + \frac{1}{2}, y + \frac{1}{2}, -z + \frac{3}{2}$.

O(hydroxy) interactions to form a supramolecular layer in the *bc*-plane, Fig. 2*a*. The layers stack along the *a* axis with no directional interactions between them, Fig. 2*b*.

4. Analysis of the Hirshfeld surfaces

Crystal Explorer 3.1 (Wolff *et al.*, 2012) was used to generate Hirshfeld surfaces mapped over d_{norm} , d_e , curvedness and electrostatic potential. The latter was calculated using *TONTTO* (Spackman *et al.*, 2008; Jayatilaka *et al.*, 2005) which was integrated into *Crystal Explorer*; the experimental geometry was used as the input. Further, the electrostatic

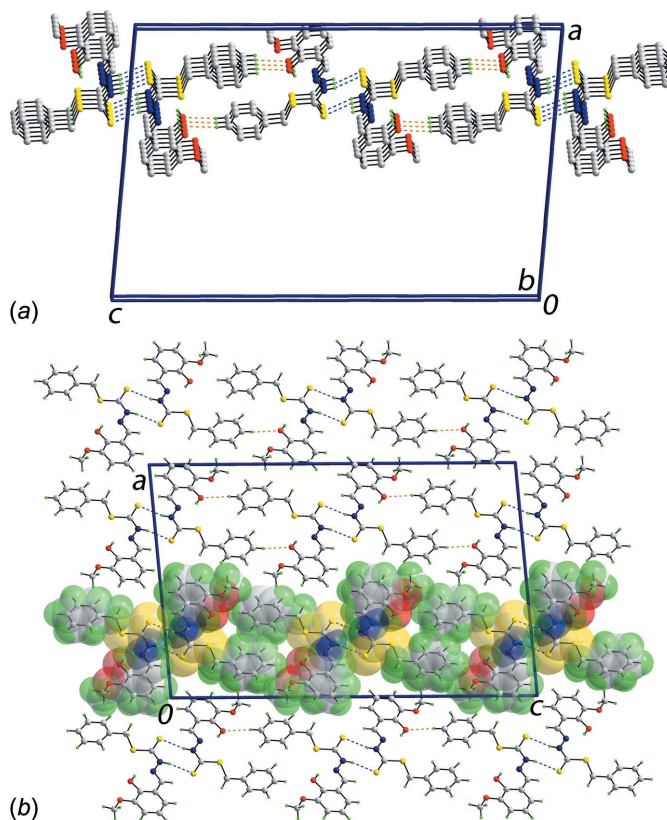


Figure 2

Molecular packing in the title compound: (a) a perspective view of the supramolecular layer sustained by thioamide-N—H···S(thione) and phenyl-C—H···O(hydroxy) interactions and, (b) a view of the unit-cell contents shown in projection down the *b* axis, highlighting one layer in space-filling mode. The N—H···S and C—H···O interactions are shown as blue and orange dashed lines, respectively. For (a), non-interacting H atoms have been omitted.

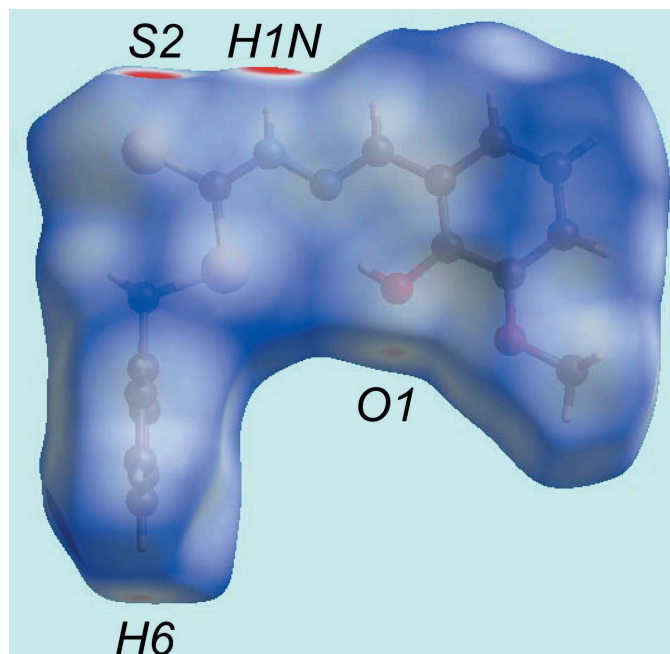


Figure 3
View of the Hirshfeld surface mapped over d_{norm} .

potentials were mapped on the Hirshfeld surface using the STO-3G basis set at the Hartree–Fock level of theory over the range ± 0.1 au. The contact distances d_i and d_e from the Hirshfeld surface to the nearest atom inside and outside, respectively, enable the analysis of the intermolecular interactions through the mapping of d_{norm} . The combination of d_e and d_i in the form of a two-dimensional fingerprint plot (Rohl *et al.*, 2008) provides a summary of the intermolecular contacts in the crystal.

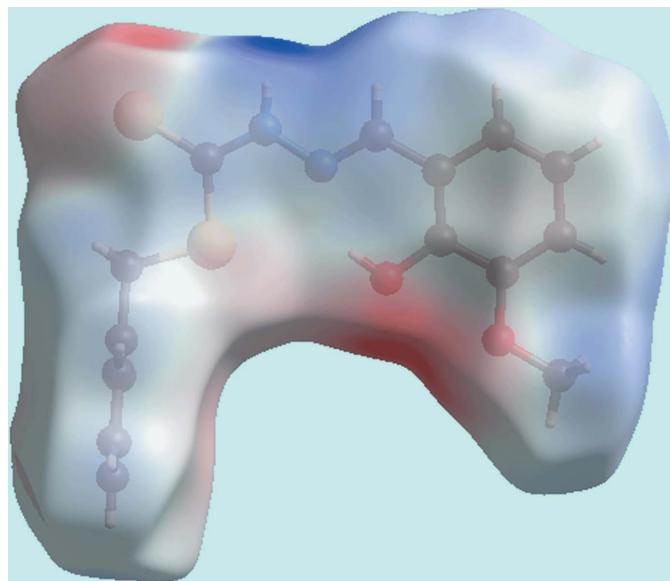


Figure 4
View of the Hirshfeld surface mapped over the electrostatic potential.

Table 2

Major percentage contribution of the different intermolecular interactions to the Hirshfeld surface of the title compound.

Contact	%
H...H	43.4
O...H/H...O	10.3
S...H/H...S	14.4
C...H/H...C	21.3
N...H/H...N	0.8
C...C	2.5
S...S	0.4
C...N/N...C	2.9
S...O/O...S	1.4
S...N/N...S	1.4
C...S/S...C	0.9

From the view of the Hirshfeld surface mapped over d_{norm} , Fig. 3, the deep-red depressions at atoms H1N and S2 confirm their role as the N—H...S hydrogen-bond donor and acceptor, respectively. On the surface mapped over the electrostatic potential, Fig. 4, these atoms appear as the respective blue and red regions. The light-red spots near the phenyl-hydrogen atom, H6, and hydroxyl oxygen, O1, on the d_{norm} -mapped surface indicate the intermolecular C—H...O interaction between them. The immediate environment about the molecule within d_{norm} -mapped Hirshfeld surface mediated by the above interactions is illustrated in Fig. 5.

The overall two-dimensional fingerprint (FP) plot, Fig. 6a, and those delineated into H...H, O...H/H...O, S...H/H...S, C...H/H...C and C...C interactions are illustrated in Fig. 6b–f; the relative contributions are summarized in Table 2. The H...H contacts appear as the scattered points in nearly the entire plot, Fig. 6b, and make a significant contribution, *i.e.* 43.4%, to the Hirshfeld surface. The round single peak at $d_e + d_i \sim 2.3$ Å results from a short interatomic H...H contact, Table 3. The FP delineated into O...H/H...O contacts show a pair of short spikes at $d_e + d_i \sim 2.5$ Å and the small arcs linked to them are identified with labels 1 and 2 in Fig. 6c. These features correspond to a 10.3% contribution to the Hirshfeld

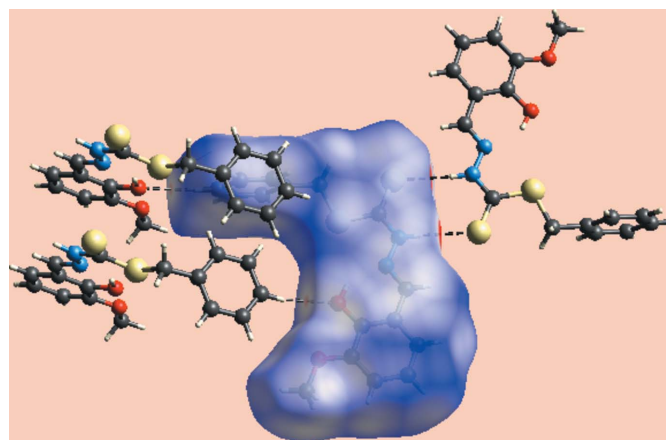


Figure 5
Hirshfeld surface mapped over d_{norm} showing hydrogen-bonding interactions with neighbouring molecules.

Table 3
Additional short interatomic contacts (Å) for the title compound.

Interaction	distance	symmetry operation
H8...H16C	2.25	$-\frac{1}{2} + x, \frac{1}{2} + y, z$
C6...H16B	2.86	$\frac{1}{2} - x, \frac{3}{2} + y, \frac{3}{2} - z$
O1...H16A	2.70	$x, 1 + y, z$
C11...H16A	2.78	$x, 1 + y, z$
C12...H16A	2.89	$x, 1 + y, z$

surfaces and reflect the presence of intermolecular C—H...O interactions as well as interatomic O...H contacts only slightly shorter than their van der Waals separation, *i.e.* around $d_e + d_i \sim 2.7$ Å, Table 3. The presence of intermolecular N—H...S hydrogen bonds in the crystal is evident from a prominent pair of sharp spikes in the outer region of the FP plot shown in Fig. 6d, *i.e.* at $d_e + d_i \sim 2.45$ Å, with a 14.4% contribution to the Hirshfeld surface. The distinct pair of wings corresponding to C...H/H...C contacts, Fig. 6e, have ‘forceps-like’ tips at $d_e + d_i \sim 2.8$ Å due to short interatomic C...H/H...C contacts, Table 3, although C—H... π interactions are not evident in the structure within the sum of their van der Waals radii. The 2.5%

Table 4
Enrichment ratios (ER) for the title compound..

Interaction	ER
H...H	0.97
O...H/H...O	1.28
S...H/H...S	1.14
C...C	1.09
C...H/H...C	1.05
S...O/O...S	1.24
S...S	0.45
C...S/S...C	0.31

contribution from C...C contacts to the Hirshfeld surface features two overlapping triangles, Fig. 6f, but the minimum ($d_e + d_i$) distance is greater than van der Waals separation, confirming the absence of π – π stacking interactions. This is also evident from the small segments delineated by blue outlines in the Hirshfeld surface mapped over curvedness, Fig. 7.

The enrichment ratio (ER), based on Hirshfeld surface analysis, gives further description of intermolecular interactions operating in a crystal (Jelsch *et al.*, 2014). The ER values are summarized in Table 4. The ER value close to but slightly less than unity, *i.e.* 0.97, for H...H contacts is in accord with expectation (Jelsch *et al.*, 2014). The sulfur atoms comprise 9.5% of Hirshfeld surface and the overall 14.4% contribution by S...H/H...S contacts results in an ER value of 1.14, which is in the expected range for N—H...S interactions, *i.e.* 1.0–1.5 (Jelsch *et al.*, 2014). The ER value of 1.28 corresponding to O...H/H...O contacts show a high propensity to form even though the percentage relative contribution to the overall surface, *i.e.* 10.3%, is small as is the 6.0% exposure provided by hydroxyl- and methoxy-oxygen atoms. The low ER value of 1.09 corresponding to C...C contacts is consistent with a low propensity for π – π stacking interactions in the

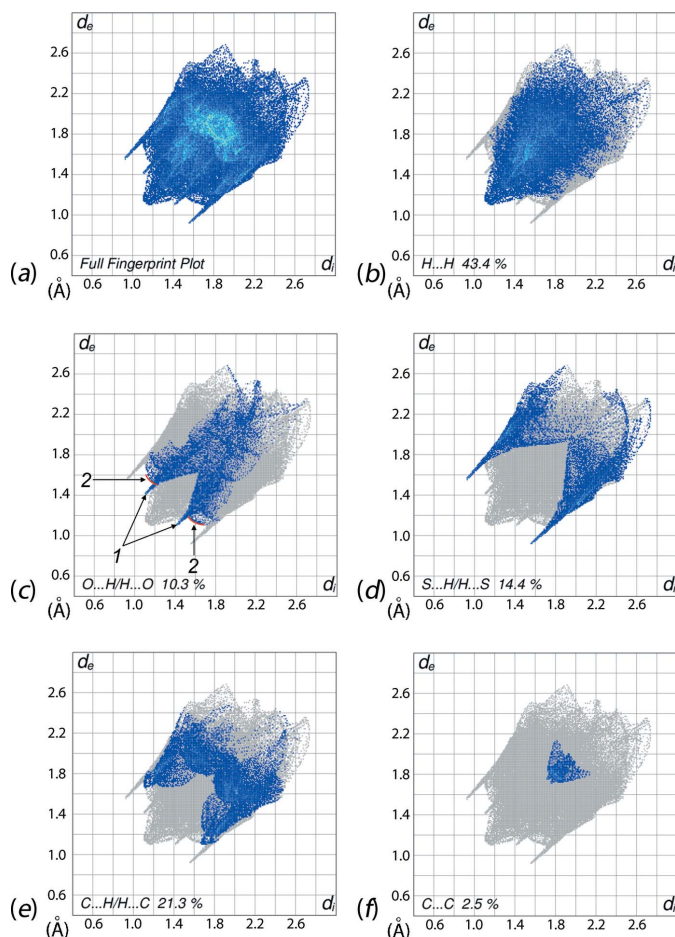


Figure 6
The two-dimensional fingerprint plots for (a) all interactions, and delineated into (b) H...H, (c) O...H/H...O, (d) S...H/H...S, (e) C...H/H...C and (f) C...C interactions.

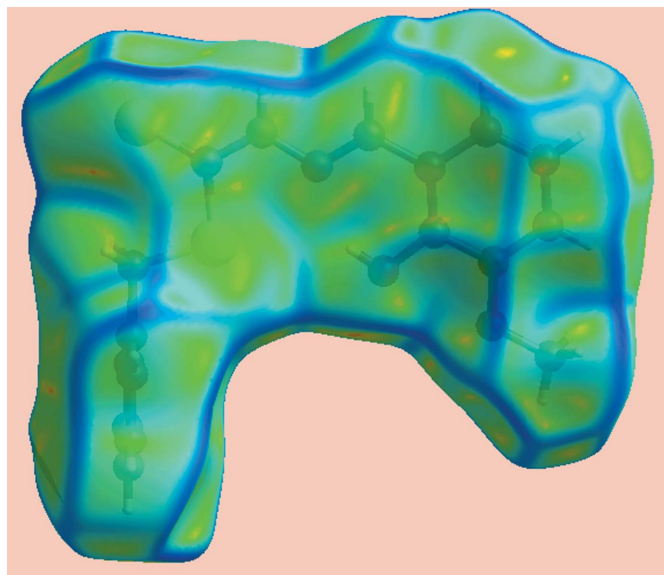
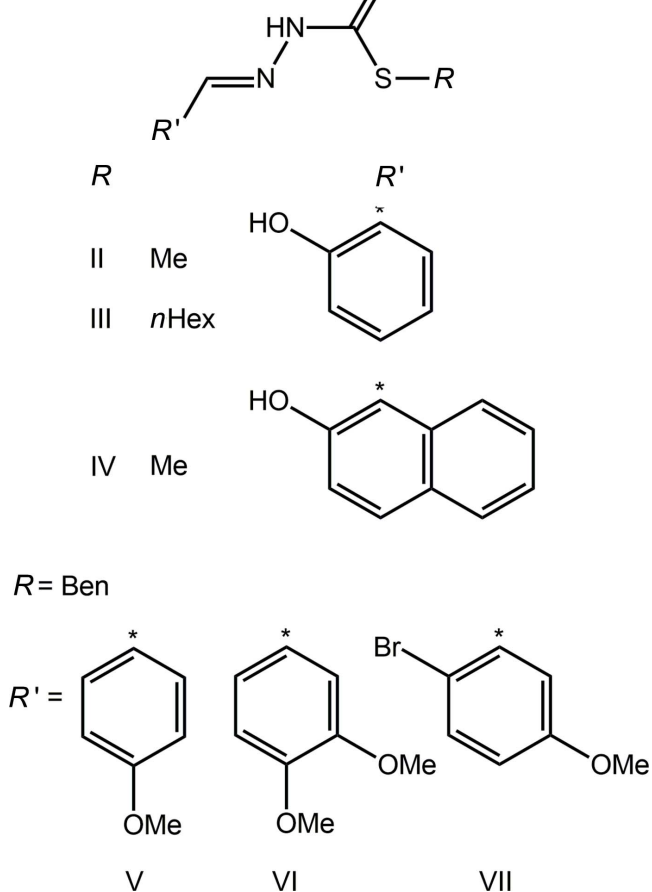


Figure 7
View of the Hirshfeld surface mapped over curvedness.

520 Yusof et al. • C₁₆H₁₆N₂O₇S₂

Crystal data	
Chemical formula	C ₁₆ H ₁₆ N ₂ O ₂ S ₂
<i>M</i> _r	332.43
Crystal system, space group	Monoclinic, <i>C2/c</i>
Temperature (K)	100
<i>a</i> , <i>b</i> , <i>c</i> (Å)	20.7896 (10), 4.6965 (2), 32.5217 (13)
β (°)	95.004 (4)
<i>V</i> (Å ³)	3163.3 (2)
<i>Z</i>	8
Radiation type	Mo Kα
μ (mm ^{−1})	0.35
Crystal size (mm)	0.25 × 0.15 × 0.07
Data collection	
Diffractometer	Agilent Xcalibur Eos Gemini
Absorption correction	Multi-scan (<i>CrysAlis PRO</i> ; Agilent, 2011)
<i>T</i> _{min} , <i>T</i> _{max}	0.87, 0.98
No. of measured, independent and observed [<i>I</i> > 2σ(<i>I</i>)] reflections	6979, 3270, 2595
<i>R</i> _{int}	0.033
(sin θ/λ) _{max} (Å ^{−1})	0.628
Refinement	
<i>R</i> [<i>F</i> ² > 2σ(<i>F</i> ²)], <i>wR</i> (<i>F</i> ²), <i>S</i>	0.041, 0.097, 1.06
No. of reflections	3270
No. of parameters	206
No. of restraints	2
H-atom treatment	H atoms treated by a mixture of independent and constrained refinement
Δρ _{max} , Δρ _{min} (e Å ^{−3})	0.33, −0.24

Acta Cryst. (2016), E72, 516–521

38.10 (CH_2). m/z calculated for $\text{C}_{16}\text{H}_{16}\text{N}_2\text{O}_2\text{S}_2$ 332.44, found 332.

7. Refinement

Crystal data, data collection and structure refinement details are summarized in Table 5. The carbon-bound H-atoms were placed in calculated positions ($\text{C}-\text{H} = 0.95\text{--}0.99\text{ \AA}$) and were included in the refinement in the riding-model approximation, with $U_{\text{iso}}(\text{H})$ set to $1.2U_{\text{eq}}(\text{C})$. The oxygen- and nitrogen-bound H-atoms were located in a difference Fourier map but were refined with distance restraints of $\text{O}-\text{H} = 0.84 \pm 0.01\text{ \AA}$ and $\text{N}-\text{H} = 0.88 \pm 0.01\text{ \AA}$, and with $U_{\text{iso}}(\text{H})$ set to $1.5U_{\text{eq}}(\text{O})$ and $1.2U_{\text{eq}}(\text{N})$.

Acknowledgements

We thank the Department of Chemistry, the Molecular Genetics Laboratory and the Department of Obstetrics and Gynaecology, Universiti Putra Malaysia, for access to facilities. This research was funded by Universiti Putra Malaysia (UPM) and the Malaysian Government under the Research University Grant Scheme (RUGS No. 9419400), the Malaysian Fundamental Research Grant Scheme (FRGS No. 01/02-13-1344FR) and the ScienceFund under the Ministry of Science, Technology and Innovation (MOSTI) (06-01-04-SF1810). ENMY also wishes to acknowledge the MyPhD Malaysian Government Scholarship (MyBrain15).

References

- Agilent (2011). *CrysAlis PRO*. Agilent Technologies, Yarnton, England.
- Ali, M. A. & Livingstone, S. E. (1974). *Coord. Chem. Rev.* **13**, 101–132.
- Ali, M. A. & Tarafder, M. T. H. (1977). *J. Inorg. Nucl. Chem.* **39**, 1785–1791.
- Basha, M. T., Chartres, J. D., Pantarat, N., Ali, M. A., Mirza, A. H., Kalinowski, D. S., Richardson, D. R. & Bernhardt, P. V. (2012). *Dalton Trans.* **41**, 6536–6548.
- Begum, M. S., Howlader, M. B. H., Sheikh, M. C., Miyatake, R. & Zangrando, E. (2016). *Acta Cryst.* **E72**, 290–292.
- Brandenburg, K. (2006). *DIAMOND*. Crystal Impact GbR, Bonn, Germany.
- Fan, Z., Huang, Y.-L., Wang, Z., Guo, H.-Q. & Shan, S. (2011a). *Acta Cryst.* **E67**, o3011.
- Fan, Z., Huang, Y.-L., Wang, Z., Guo, H.-Q. & Shan, S. (2011b). *Acta Cryst.* **E67**, o3015.
- Farrugia, L. J. (2012). *J. Appl. Cryst.* **45**, 849–854.
- Groom, C. R. & Allen, F. H. (2014). *Angew. Chem. Int. Ed.* **53**, 662–671.
- Jayatilaka, D., Grimwood, D. J., Lee, A., Lemay, A., Russel, A. J., Taylor, C., Wolff, S. K., Cassam-Chenai, P. & Whitton, A. (2005). *TONTO*. Available at: <http://hirshfeldsurface.net/>
- Jelsch, C., Ejsmont, K. & Huder, L. (2014). *IUCrJ*, **1**, 119–128.
- Liu, Z., Wang, W., Xu, H., Sheng, L., Chen, S., Huang, D. & Sun, F. (2015). *Inorg. Chem. Commun.* **62**, 19–23.
- Madanhire, T., Abrahams, A., Hosten, E. C. & Betz, R. (2015). *Z. Kristallogr. New Cryst. Struct.* **230**, 13–14.
- Rohl, A. L., Moret, M., Kaminsky, W., Claborn, K., McKinnon, J. J. & Kahr, B. (2008). *Cryst. Growth Des.* **8**, 4517–4525.
- Sethuraman, G., Yamin, B. M., Shamsuddin, M., Usman, A., Razak, I. A. & Fun, H.-K. (2002). *Acta Cryst.* **E58**, o649–o651.
- Sheldrick, G. M. (2008). *Acta Cryst.* **A64**, 112–122.
- Sheldrick, G. M. (2015). *Acta Cryst.* **C71**, 3–8.
- Spackman, M. A., McKinnon, J. J. & Jayatilaka, D. (2008). *CrystEngComm*, **10**, 377–388.
- Tan, Y.-F., Break, M. K. bin, Tahir, M. I. M. & Khoo, T.-J. (2015). *Acta Cryst.* **E71**, 238–240.
- Vijayan, P., Viswanathamurthi, P., Sugumar, P., Ponnuswamy, M. N., Balakumaran, M. D., Kalaichelvan, P. T., Velmurugan, K., Nandhakumar, R. & Butcher, R. J. (2015). *Inorg. Chem. Front.* **2**, 620–639.
- Westrip, S. P. (2010). *J. Appl. Cryst.* **43**, 920–925.
- Wise, C. F., Liu, D., Mayer, K. J., Crossland, P. M., Hartley, C. L. & McNamara, W. R. (2015). *Dalton Trans.* **44**, 14265–14271.
- Wolff, S. K., Grimwood, D. J., McKinnon, J. J., Turner, M. J., Jayatilaka, D. & Spackman, M. A. (2012). *Crystal Explorer*. The University of Western Australia.
- Yusof, E. N. M., Ravoo, T. B. S. A., Jamsari, J., Tiekink, E. R. T., Veerakumarasivam, A., Crouse, K. A., Tahir, M. I. M. & Ahmad, H. (2015). *Inorg. Chim. Acta*, **438**, 85–93.
- Yusof, E. N. M., Ravoo, T. B. S. A., Tiekink, E. R. T., Veerakumarasivam, A., Crouse, K. A., Tahir, M. I. M. & Ahmad, H. (2015). *Int. J. Molec. Sci.* **16**, 11034–11054.

supporting information

Acta Cryst. (2016). E72, 516-521 [https://doi.org/10.1107/S2056989016004291]

2-[(1*E*)-{[(Benzylsulfanyl)methanethioyl]amino}imino)methyl]-6-methoxyphenol: crystal structure and Hirshfeld surface analysis

Enis Nadia Md Yusof, Mukesh M. Jotani, Edward R. T. Tiekink and Thahira B. S. A. Ravooof

Computing details

Data collection: *CrysAlis PRO* (Agilent, 2011); cell refinement: *CrysAlis PRO* (Agilent, 2011); data reduction: *CrysAlis PRO* (Agilent, 2011); program(s) used to solve structure: *SHELXS97* (Sheldrick, 2008); program(s) used to refine structure: *SHELXL2014* (Sheldrick, 2015); molecular graphics: *ORTEP-3 for Windows* (Farrugia, 2012) and *DIAMOND* (Brandenburg, 2006); software used to prepare material for publication: *publCIF* (Westrip, 2010).

2-[(1*E*)-{[(Benzylsulfanyl)methanethioyl]amino}imino)methyl]-6-methoxyphenol

Crystal data

$C_{16}H_{16}N_2O_2S_2$

$M_r = 332.43$

Monoclinic, $C2/c$

$a = 20.7896$ (10) Å

$b = 4.6965$ (2) Å

$c = 32.5217$ (13) Å

$\beta = 95.004$ (4)°

$V = 3163.3$ (2) Å³

$Z = 8$

$F(000) = 1392$

$D_x = 1.396$ Mg m⁻³

Mo $K\alpha$ radiation, $\lambda = 0.71073$ Å

Cell parameters from 2185 reflections

$\theta = 2-29^\circ$

$\mu = 0.35$ mm⁻¹

$T = 100$ K

Plate, light-yellow

$0.25 \times 0.15 \times 0.07$ mm

Data collection

Agilent Xcalibur Eos Gemini
diffractometer

Radiation source: Enhance (Mo) X-ray Source

Graphite monochromator

Detector resolution: 16.1952 pixels mm⁻¹

ω scans

Absorption correction: multi-scan
(*CrysAlis PRO*; Agilent, 2011)

$T_{\min} = 0.87$, $T_{\max} = 0.98$

6979 measured reflections

3270 independent reflections

2595 reflections with $I > 2\sigma(I)$

$R_{\text{int}} = 0.033$

$\theta_{\max} = 26.5^\circ$, $\theta_{\min} = 2.4^\circ$

$h = -25 \rightarrow 26$

$k = -5 \rightarrow 5$

$l = -27 \rightarrow 40$

Refinement

Refinement on F^2

Least-squares matrix: full

$R[F^2 > 2\sigma(F^2)] = 0.041$

$wR(F^2) = 0.097$

$S = 1.06$

3270 reflections

206 parameters

2 restraints

H atoms treated by a mixture of independent
and constrained refinement

$w = 1/[\sigma^2(F_o^2) + (0.0382P)^2 + 1.7624P]$

where $P = (F_o^2 + 2F_c^2)/3$

$(\Delta/\sigma)_{\max} = 0.002$

$\Delta\rho_{\max} = 0.33$ e Å⁻³

$\Delta\rho_{\min} = -0.24$ e Å⁻³

Special details

Geometry. All esds (except the esd in the dihedral angle between two l.s. planes) are estimated using the full covariance matrix. The cell esds are taken into account individually in the estimation of esds in distances, angles and torsion angles; correlations between esds in cell parameters are only used when they are defined by crystal symmetry. An approximate (isotropic) treatment of cell esds is used for estimating esds involving l.s. planes.

Fractional atomic coordinates and isotropic or equivalent isotropic displacement parameters (\AA^2)

	<i>x</i>	<i>y</i>	<i>z</i>	$U_{\text{iso}}^*/U_{\text{eq}}$
S1	0.22247 (2)	0.46299 (12)	0.61684 (2)	0.02185 (15)
S2	0.17478 (3)	0.80851 (12)	0.54164 (2)	0.02258 (15)
O1	0.35672 (7)	−0.0373 (3)	0.63252 (4)	0.0239 (3)
H1O	0.3342 (10)	0.086 (4)	0.6194 (7)	0.036*
O2	0.43677 (8)	−0.4115 (3)	0.66547 (5)	0.0305 (4)
N1	0.27458 (8)	0.4630 (4)	0.54712 (5)	0.0203 (4)
H1N	0.2819 (10)	0.519 (5)	0.5223 (4)	0.024*
N2	0.31479 (8)	0.2682 (4)	0.56753 (5)	0.0194 (4)
C1	0.22604 (9)	0.5777 (4)	0.56594 (6)	0.0179 (4)
C2	0.15287 (10)	0.6579 (5)	0.63209 (6)	0.0237 (5)
H2A	0.1579	0.8639	0.6268	0.028*
H2B	0.1130	0.5907	0.6161	0.028*
C3	0.14873 (10)	0.6059 (5)	0.67741 (6)	0.0223 (5)
C4	0.18779 (13)	0.7499 (6)	0.70649 (8)	0.0395 (6)
H4	0.2181	0.8838	0.6979	0.047*
C5	0.18365 (13)	0.7029 (6)	0.74845 (8)	0.0432 (7)
H5	0.2108	0.8059	0.7682	0.052*
C6	0.14056 (12)	0.5086 (5)	0.76139 (7)	0.0356 (6)
H6	0.1381	0.4735	0.7900	0.043*
C7	0.10141 (14)	0.3670 (7)	0.73262 (8)	0.0502 (8)
H7	0.0708	0.2346	0.7413	0.060*
C8	0.10538 (13)	0.4127 (6)	0.69076 (8)	0.0404 (7)
H8	0.0779	0.3096	0.6712	0.048*
C9	0.35930 (10)	0.1553 (4)	0.54759 (6)	0.0192 (4)
H9	0.3635	0.2118	0.5199	0.023*
C10	0.40308 (9)	−0.0564 (4)	0.56664 (6)	0.0188 (4)
C11	0.40002 (9)	−0.1423 (4)	0.60766 (6)	0.0191 (4)
C12	0.44376 (10)	−0.3469 (5)	0.62508 (7)	0.0236 (5)
C13	0.48986 (10)	−0.4610 (5)	0.60167 (7)	0.0282 (5)
H13	0.5196	−0.5984	0.6134	0.034*
C14	0.49292 (11)	−0.3747 (5)	0.56070 (7)	0.0286 (5)
H14	0.5246	−0.4541	0.5448	0.034*
C15	0.45042 (10)	−0.1762 (5)	0.54345 (7)	0.0239 (5)
H15	0.4529	−0.1189	0.5156	0.029*
C16	0.47583 (12)	−0.6366 (5)	0.68359 (8)	0.0346 (6)
H16A	0.4679	−0.8109	0.6674	0.052*
H16B	0.4649	−0.6693	0.7119	0.052*
H16C	0.5215	−0.5840	0.6839	0.052*

Atomic displacement parameters (\AA^2)

	U^{11}	U^{22}	U^{33}	U^{12}	U^{13}	U^{23}
S1	0.0221 (3)	0.0271 (3)	0.0169 (3)	0.0071 (2)	0.0051 (2)	0.0040 (2)
S2	0.0225 (3)	0.0273 (3)	0.0180 (3)	0.0075 (2)	0.0024 (2)	0.0047 (2)
O1	0.0258 (8)	0.0281 (9)	0.0183 (7)	0.0072 (7)	0.0044 (6)	0.0034 (7)
O2	0.0399 (9)	0.0269 (9)	0.0238 (8)	0.0075 (7)	−0.0035 (7)	0.0064 (7)
N1	0.0206 (9)	0.0253 (10)	0.0154 (8)	0.0044 (8)	0.0040 (7)	0.0058 (8)
N2	0.0180 (8)	0.0208 (9)	0.0194 (9)	0.0039 (7)	0.0024 (7)	0.0026 (8)
C1	0.0181 (10)	0.0179 (10)	0.0176 (10)	−0.0018 (8)	0.0016 (8)	0.0000 (9)
C2	0.0239 (11)	0.0257 (12)	0.0222 (11)	0.0080 (9)	0.0061 (9)	0.0038 (10)
C3	0.0234 (11)	0.0231 (12)	0.0212 (11)	0.0093 (9)	0.0059 (9)	0.0005 (9)
C4	0.0430 (15)	0.0457 (16)	0.0293 (13)	−0.0093 (13)	0.0010 (12)	0.0040 (12)
C5	0.0523 (17)	0.0504 (17)	0.0258 (13)	−0.0002 (14)	−0.0034 (12)	−0.0029 (13)
C6	0.0411 (14)	0.0470 (16)	0.0200 (11)	0.0152 (12)	0.0103 (11)	0.0032 (12)
C7	0.0549 (18)	0.066 (2)	0.0310 (14)	−0.0188 (16)	0.0104 (13)	0.0078 (14)
C8	0.0493 (16)	0.0480 (16)	0.0244 (12)	−0.0172 (13)	0.0063 (12)	−0.0001 (12)
C9	0.0225 (10)	0.0203 (11)	0.0150 (10)	−0.0017 (9)	0.0028 (9)	0.0010 (9)
C10	0.0184 (10)	0.0170 (10)	0.0210 (10)	−0.0013 (9)	0.0015 (8)	−0.0030 (9)
C11	0.0185 (10)	0.0189 (11)	0.0197 (10)	−0.0013 (8)	0.0004 (9)	−0.0039 (9)
C12	0.0264 (11)	0.0194 (11)	0.0239 (11)	−0.0004 (9)	−0.0046 (9)	−0.0011 (9)
C13	0.0239 (11)	0.0238 (12)	0.0355 (13)	0.0068 (10)	−0.0067 (10)	−0.0046 (11)
C14	0.0228 (11)	0.0301 (13)	0.0331 (13)	0.0063 (10)	0.0035 (10)	−0.0077 (11)
C15	0.0223 (11)	0.0269 (12)	0.0228 (11)	0.0012 (9)	0.0041 (9)	−0.0030 (10)
C16	0.0411 (14)	0.0237 (13)	0.0363 (14)	−0.0008 (11)	−0.0129 (12)	0.0070 (11)

Geometric parameters (\AA , $^\circ$)

S1—C1	1.749 (2)	C6—C7	1.359 (4)
S1—C2	1.817 (2)	C6—H6	0.9500
S2—C1	1.670 (2)	C7—C8	1.388 (3)
O1—C11	1.354 (2)	C7—H7	0.9500
O1—H1O	0.836 (10)	C8—H8	0.9500
O2—C12	1.368 (3)	C9—C10	1.450 (3)
O2—C16	1.429 (3)	C9—H9	0.9500
N1—C1	1.338 (2)	C10—C11	1.401 (3)
N1—N2	1.371 (2)	C10—C15	1.408 (3)
N1—H1N	0.874 (9)	C11—C12	1.408 (3)
N2—C9	1.290 (2)	C12—C13	1.383 (3)
C2—C3	1.504 (3)	C13—C14	1.400 (3)
C2—H2A	0.9900	C13—H13	0.9500
C2—H2B	0.9900	C14—C15	1.370 (3)
C3—C4	1.370 (3)	C14—H14	0.9500
C3—C8	1.376 (3)	C15—H15	0.9500
C4—C5	1.392 (3)	C16—H16A	0.9800
C4—H4	0.9500	C16—H16B	0.9800
C5—C6	1.370 (4)	C16—H16C	0.9800
C5—H5	0.9500		

C1—S1—C2	101.75 (10)	C3—C8—C7	120.5 (2)
C11—O1—H1O	108.6 (16)	C3—C8—H8	119.7
C12—O2—C16	117.13 (17)	C7—C8—H8	119.7
C1—N1—N2	119.96 (16)	N2—C9—C10	121.21 (18)
C1—N1—H1N	120.0 (15)	N2—C9—H9	119.4
N2—N1—H1N	120.0 (15)	C10—C9—H9	119.4
C9—N2—N1	117.70 (17)	C11—C10—C15	119.1 (2)
N1—C1—S2	121.37 (15)	C11—C10—C9	121.72 (18)
N1—C1—S1	113.89 (15)	C15—C10—C9	119.15 (18)
S2—C1—S1	124.74 (11)	O1—C11—C10	123.47 (19)
C3—C2—S1	107.49 (14)	O1—C11—C12	116.60 (18)
C3—C2—H2A	110.2	C10—C11—C12	119.92 (18)
S1—C2—H2A	110.2	O2—C12—C13	125.4 (2)
C3—C2—H2B	110.2	O2—C12—C11	114.77 (18)
S1—C2—H2B	110.2	C13—C12—C11	119.8 (2)
H2A—C2—H2B	108.5	C12—C13—C14	120.2 (2)
C4—C3—C8	118.2 (2)	C12—C13—H13	119.9
C4—C3—C2	121.0 (2)	C14—C13—H13	119.9
C8—C3—C2	120.8 (2)	C15—C14—C13	120.4 (2)
C3—C4—C5	121.0 (2)	C15—C14—H14	119.8
C3—C4—H4	119.5	C13—C14—H14	119.8
C5—C4—H4	119.5	C14—C15—C10	120.6 (2)
C6—C5—C4	120.3 (3)	C14—C15—H15	119.7
C6—C5—H5	119.8	C10—C15—H15	119.7
C4—C5—H5	119.8	O2—C16—H16A	109.5
C7—C6—C5	118.8 (2)	O2—C16—H16B	109.5
C7—C6—H6	120.6	H16A—C16—H16B	109.5
C5—C6—H6	120.6	O2—C16—H16C	109.5
C6—C7—C8	121.1 (3)	H16A—C16—H16C	109.5
C6—C7—H7	119.4	H16B—C16—H16C	109.5
C8—C7—H7	119.4		

Hydrogen-bond geometry (\AA , $^\circ$)

$D-H\cdots A$	$D-H$	$H\cdots A$	$D\cdots A$	$D-H\cdots A$
O1—H1O \cdots N2	0.84 (2)	1.90 (2)	2.639 (2)	146 (2)
N1—H1N \cdots S2 ⁱ	0.88 (2)	2.47 (2)	3.3351 (18)	168 (2)
C6—H6 \cdots O1 ⁱⁱ	0.95	2.51	3.453 (3)	170

Symmetry codes: (i) $-x+1/2, -y+3/2, -z+1$; (ii) $-x+1/2, y+1/2, -z+3/2$.